

Figure 2. Distribution of optical coherence tomography (OCT) macular map grid points correlated with visual acuity (VA). The greyscale maps show the correlation coefficient of VA and the thickness of the retinal nerve fibre layer (RNFL) (a), ganglion cell complex (GCC) (b), and ganglion cell layer plus inner plexiform layer (GCL + IPL) (c). The right side of the figure represents the nasal (the disc side) and the left side represents the temporal. Darker shades of grey indicate a higher correlation coefficient, with a step scale of 0.1. Grid points shown in white had no statistically significant correlation.

correlated grid points were round and centered in the upper nasal region, which includes the PMB. In the GCL + IPL map, the correlation coefficient with VA ranged from -0.31 to -0.51. The correlated area in this map was flatter and closer to the PMB.

In the current study, we obtained data on the regional correlation of HFA 10-2 test points and the OCT macular map to VA in OAG patients. We found that areas with higher correlation ($r > 0.4$) were mainly located in the PMB. In a previous study, we demonstrated that cpRNFLT

in the temporal region, which includes the PMB, was significantly correlated to VA ($r = -0.4$) in patients with OAG.³ We also found that the pathogenesis of this decreased VA may be related to myopia and decreased tissue blood flow in the temporal optic disc.³ Interestingly, other research has found that patients with strong fluctuations in ocular perfusion pressure (OPP) also undergo significant progressive loss of macular function.⁴ Decreased macular function is thus implicated in glaucoma, and decreased OPP may also be related to the pathogenesis of central VF deterioration.

In conclusion, we found that in patients with glaucoma, VA was strongly correlated to HFA 10-2 and the OCT macular map in the PMB area, suggesting that the analysis of regional data from the HFA 10-2 or OCT macular map may be a useful diagnostic tool in glaucoma patients with decreased VA. These findings also suggest that the involvement of the PMB in glaucomatous damage may make it a useful biomarker of significantly deteriorated QOL.

ACKNOWLEDGEMENTS

The authors thank Mr Tim Hilts for editing this manuscript and Dr Masahiro Akiba for useful discussion.

Kazuko Omodaka MD,¹ Takeshi Yabana MD,¹
Naoko Takada MD¹ and
Toru Nakazawa MD PhD^{1,2,3}

Departments of ¹Ophthalmology, ²Retinal Disease Control
and ³Advanced Ophthalmic Medicine, Tohoku University
Graduate School of Medicine, Sendai, Japan

Received 7 July 2014; accepted 15 July 2014.

REFERENCES

1. Murata H, Hirasawa H, Aoyama Y *et al.* Identifying areas of the visual field important for quality of life in patients with glaucoma. *PLoS ONE* 2013; **8**: e58695.
2. Hood DC, Raza AS, de Moraes CG, Liebmann JM, Ritch R. Glaucomatous damage of the macula. *Prog Retin Eye Res* 2013; **32**: 1–21.
3. Omodaka K, Nakazawa T, Yokoyama Y, Doi H, Fuse N, Nishida K. Correlation between peripapillary macular fiber layer thickness and visual acuity in patients with open-angle glaucoma. *Clin Ophthalmol* 2010; **4**: 629–35.
4. Choi J, Lee JR, Lee Y *et al.* Relationship between 24-hour mean ocular perfusion pressure fluctuation and rate of paracentral visual field progression in normal-tension glaucoma. *Invest Ophthalmol Vis Sci* 2013; **54**: 6150–57.

Citation analysis of the most- and least-cited articles in *Clinical and Experimental Ophthalmology*: 2000–2013

Citation analysis has become a key tool used to judge and quantify the impact of scientific literature.^{1,2} The funda-

mental measure is the journal citation count that assesses the frequency with which a published article is cited in the scientific literature.¹ To ascertain whether differences between most-cited and least-cited articles can be identified, we analysed the characteristics of the most- and least-cited articles in *Clinical and Experimental Ophthalmology* (CEO).

A core search was conducted (26 February 2014) via the Web of Science database (<http://thomsonreuters.com/thomson-reuters-web-of-science/>) for '*Clinical and Experimental Ophthalmology*' publications 2000–2013 (the journal was launched in 2000). To avoid inclusion of extraneous material, the search was refined by the primary journal document types 'Article', 'Letter', 'Editorial' and 'Review'. From 2355 articles identified (1434 original articles, 555 letters, 260 editorials and 106 reviews), a citation report was generated and ordered according to total citations received.

The 100 most-cited and 100 least-cited articles were analysed in terms of title, authors, year published, country, keywords, subject category, total citations and average citations per year. For simplicity, the corresponding author's institution determined country of origin. Subject categories were allocated according to the core theme and selected keywords, including: anterior segment, glaucoma, neuro-ophthalmology, visual sciences, uveitis, medical retinal, vitreoretinal, ocular genetics, ocular oncology, ophthalmic pharmacotherapy, oculoplastics and humanities. The 100 most-cited articles were determined by the number of total citations accrued. The 100 least-cited articles were identified from those that received zero citation in chronological order starting from year 2000.

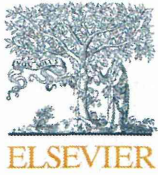
The top 20 most-cited articles are listed in Table 1 (top 100 available as Supporting information – online only). The most-cited article, by Young *et al.* (2000) had accrued 233 citations.³ Research groups featuring most prominently in the top 100 most-cited articles included those of Mitchell (Sydney) and McGhee (Auckland) – affiliated with eight and seven articles, respectively. Anterior segment and visual science topics were the most popular subject categories in the top 100.

The average total citation count in the top 100 most-cited articles was 44.4 (range 27–233) with 4.3 (range 1.9–16.6) average annual citations. Interestingly, articles in the most-cited group had on average twice the number of authors (4.82)^{1–9} compared with the least-cited group (2.28)^{1–8}. Single-author articles were more prevalent in the least-cited group (43) than in the most-cited group (6). Both groups comprised articles from an array of countries (Table 2). Australia produced the greatest number of articles at 47% and 47%, followed by New Zealand at 12% and 14%, in the most-cited and least-cited groups, respectively.

Perhaps unsurprisingly, original articles were well-represented in the most-cited 100 (75%), and underrepresented in the least-cited 100 (34%), compared with overall journal representation (61%). Notably, although reviews represented only 4% of journal output, 22% of the most-cited articles were reviews. In contrast, editorials and 'letters to the editor' represented a significant proportion of

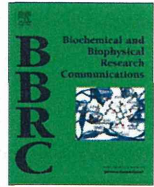
Competing/conflicts of interest: No stated conflict of interest

Funding sources: No stated funding sources



Contents lists available at ScienceDirect

Biochemical and Biophysical Research Communications

journal homepage: www.elsevier.com/locate/ybbrc

The role of calpain in an *in vivo* model of oxidative stress-induced retinal ganglion cell damage



Yu Yokoyama^a, Kazuichi Maruyama^a, Kotaro Yamamoto^a, Kazuko Omodaka^a, Masayuki Yasuda^a, Noriko Himori^a, Morin Ryu^a, Koji M. Nishiguchi^a, Toru Nakazawa^{a,b,c,*}

^a Department of Ophthalmology, Tohoku University Graduate School of Medicine, Miyagi, Japan

^b Department of Retinal Disease Control, Tohoku University Graduate School of Medicine, Miyagi, Japan

^c Department of Advanced Ophthalmic Medicine, Tohoku University Graduate School of Medicine, Miyagi, Japan

ARTICLE INFO

Article history:

Received 29 July 2014

Available online 8 August 2014

Keywords:

Retinal ganglion cell

Oxidative stress

Apoptosis

Calpain

AAPH

SNJ-1945

ABSTRACT

Purpose: In this study, we set out to establish an *in vivo* animal model of oxidative stress in the retinal ganglion cells (RGCs) and determine whether there is a link between oxidative stress in the RGCs and the activation of calpain, a major part of the apoptotic pathway.

Materials and methods: Oxidative stress was induced in the RGCs of C57BL/6 mice by the intravitreal administration of 2,2'-azobis (2-amidinopropane) dihydrochloride (AAPH, 30 mM, 2 μ l). Control eyes were injected with 2 μ l of vehicle. Surviving Fluorogold (FG)-labeled RGCs were then counted in retinal flat mounts. Double staining with CellROX and Annexin V was performed to investigate the co-localization of free radical generation and apoptosis. An immunoblot assay was used both to indirectly evaluate calpain activation in the AAPH-treated eyes by confirming α -fodrin cleavage, and also to evaluate the effect of SNJ-1945 (a specific calpain inhibitor: 4% w/v, 100 mg/kg, intraperitoneal administration) in these eyes.

Results: Intravitreal administration of AAPH led to a significant decrease in FG-labeled RGCs 7 days after treatment (control: 3806.7 ± 575.2 RGCs/mm², AAPH: 3156.1 ± 371.2 RGCs/mm², $P < 0.01$). CellROX and Annexin V signals were co-localized in the FG-labeled RGCs 24 h after AAPH injection. An immunoblot assay revealed a cleaved α -fodrin band that increased significantly 24 h after AAPH administration. Intraperitoneally administered SNJ-1945 prevented the cleavage of α -fodrin and had a neuroprotective effect against AAPH-induced RGC death (AAPH: 3354.0 ± 226.9 RGCs/mm², AAPH+SNJ-1945: 3717.1 ± 614.6 RGCs/mm², $P < 0.01$).

Conclusion: AAPH administration was an effective model of oxidative stress in the RGCs, showing that oxidative stress directly activated the calpain pathway and induced RGC death. Furthermore, inhibition of the calpain pathway protected the RGCs after AAPH administration.

© 2014 Elsevier Inc. All rights reserved.

1. Introduction

Optic nerve fiber degeneration resulting in retinal ganglion cell (RGC) death, which occurs in diseases such as glaucoma, can threaten visual function and lead to blindness. Various studies have investigated possible treatments aimed at preventing this process, but the pathological mechanism of optic nerve degeneration and

RGC loss is not yet well understood. Thus, viable neuroprotective strategies have not yet been found.

Many neuroprotective strategies have been considered so far. Among the most promising are those targeting oxidative stress, which is associated with aging. Oxidative stress has a role in the pathogenesis of various systemic diseases, and is known to induce neuronal cell death in neurodegenerative diseases such as Alzheimer's disease, amyotrophic lateral sclerosis, and Parkinson's disease [1–3]. Oxidative stress has also been implicated in glaucoma, and it is necessary to better understand the underlying mechanism of oxidative stress-induced dysfunction in order to more effectively treat this disease [4,5]. Recently, a number of studies demonstrated that optic nerve crush (NC), a commonly used model of the axonal injury that occurs in ocular diseases such as glaucoma, could help elucidate the cytotoxic role of oxidative

Abbreviations: RGC, retinal ganglion cell; AAPH, 2,2'-azobis (2-amidinopropane) dihydrochloride; FG, Fluorogold; NC, optic nerve crush; Ca²⁺, calcium ion; DPBS, Dulbecco's phosphate-buffered saline; PFA, paraformaldehyde; CMC, carboxymethylcellulose; ROS, reactive oxygen species; AIF, apoptosis-inducing factor.

* Corresponding author at: Department of Ophthalmology, Tohoku University Graduate School of Medicine, 1-1, Seiryō, Aoba, Sendai, Miyagi 980-8574, Japan. Fax: +81 22 717 7298.

E-mail address: ntoru@oph.med.tohoku.ac.jp (T. Nakazawa).

<http://dx.doi.org/10.1016/j.bbrc.2014.08.009>

0006-291X/© 2014 Elsevier Inc. All rights reserved.

stress in the process of RGC death [6,7]. In a previous study, we showed that mice deficient in Nrf2, a key transcription factor regulating the expression of anti-oxidant genes, had significantly fewer surviving Fluorogold (FG)-labeled RGCs than wild-type mice 7 days after NC. This result suggested that the regulation of oxidative stress signaling was a potential neuroprotective treatment for diseases affecting the optic nerve fiber and the RGCs.

Our previous research showed that the activation of calpain played a key role in the process of RGC death after NC [7]. Calpain is a member of the cysteine protease family that is regulated by increased intracellular calcium ion (Ca^{2+}) levels and is raised locally through calcium channels. A large Ca^{2+} influx into the cytosol leads to calpain activation and cell death in various pathological conditions [8–10]. However, although our previous studies showed that NC caused oxidative stress and calpain activation in the retina *in vivo*, NC is a model of axonal injury generally, not oxidative stress specifically, and therefore cannot serve as a method of directly evaluating the efficacy of neuroprotective strategies against oxidative stress.

Therefore, to directly explore the effect of oxidative stress on calpain activation, we established a new *in vivo* mouse model of RGC degeneration caused by oxidative stress, using the intravitreal administration of 2,2'-azobis (2-amidinopropane) dihydrochloride (AAPH) [11]. In this report, we use this model to attempt to determine whether the calpain pathway has a causative role in oxidative damage-induced RGC death, and whether inhibiting oxidative stress-induced calpain activation has potential as a neuroprotective treatment for ocular diseases involving oxidative stress.

2. Materials and methods

This study used adult (10–12-week old) male C57BL/6 mice (SLC, Shizuoka, Japan). All animals were maintained and handled in accordance with the ARVO Statement for the Use of Animals in Ophthalmic and Vision Research and the guidelines from the Declaration of Helsinki and Guiding Principles in the Care and Use of Animals. All experimental procedures described in the present study were approved by the Ethics Committee for Animal Experiments at Tohoku University Graduate School of Medicine.

2.1. Induction of oxidative stress in the retina

Intravitreal administration of AAPH was performed as previously described [12–14]. Briefly, each animal was anesthetized with pentobarbital (50 mg/kg). Two microliters of AAPH (30 mM) was injected intravitreally using a Hamilton syringe with a 32 G needle under surgical stereomicroscopy. The same volume of Dulbecco's phosphate-buffered saline (DPBS) was injected in the control group. If lens injuries or vitreous hemorrhaging were observed after the injection, the animals were excluded from the study.

2.2. Retrograde labeling of the RGCs and cell counting

Retrograde labeling was performed as described previously using a fluorescent tracer, FG (Fluorochrome, LLC, Denver, CO, USA), 7 days before the intravitreal injection of AAPH or DPBS [12]. Briefly, the mice were anesthetized with a mixture of ketamine (100 mg/kg) and xylazine (9 mg/kg) prepared at room temperature. Under full anesthesia, two small holes were drilled into the skull at sites corresponding to the superior colliculi, and 2 μl of 2% FG with 1% dimethylsulfoxide were injected using a Hamilton syringe with a 32 G needle. Seven days after the intravitreal injection of AAPH or DPBS, the retinas were harvested and fixed with 4% paraformaldehyde (PFA) for three hours. The retinas were then placed on glass slides with the ganglion cell layer facing up. Vecta-

shield mounting medium (Vector Laboratories) and a cover glass were also applied. RGC survival was determined by counting FG-labeled RGCs in 12 distinct areas under the microscope [12]. Our investigation of the effect of calpain used the calpain inhibitor SNJ-1945 (Senju Pharmaceutical Co., Ltd). One day before administration of AAPH, the FG-labeled mice received an intraperitoneal administration of 4% w/v SNJ-1945 (100 mg/kg) in carboxymethylcellulose (CMC). The control group received CMC without SNJ-1945. Administration of SNJ-1945 continued daily until 7 days after the AAPH injection, when the retinas were harvested. Fixation of the retinas and RGC counting were then performed as described above.

2.3. Immunoblot assay

Immunoblotting was performed as previously described with minor modifications [13,14]. Isolated retinas were obtained surgically 3, 6 and 24 h after the intravitreal injection of AAPH or DPBS and placed in a lysis buffer (25 mM Tris-HCl; pH 7.6, 150 mM NaCl, 1% NP-40, 1% sodium deoxycholate, 0.1% SDS, 1% protease inhibitor cocktail; Sigma-Aldrich, 1% phosphatase inhibitor cocktail 2; Sigma-Aldrich). Each sample was separated with SDS-PAGE and electroblotted to polyvinylidene fluoride membranes (Immobilon-P, Millipore). After blocking the membrane with 4% BlockAce (Yukijirushi), they were incubated with primary mouse monoclonal antibodies against α -fodrin (1:750, Abcam), and β -actin (1:5000, Sigma-Aldrich) overnight at 4 °C. The membranes were then incubated with a horseradish peroxidase-conjugated goat immunoglobulin secondary antibody. Detection of the antigen-antibody complex was performed with the ECL Prime Western Blotting Detection System (GE Healthcare). Signals were measured in Image Lab statistical software (Bio-Rad, Hercules, CA, USA) and normalized to β -actin.

2.4. Detection of free radicals and RGC apoptosis

Staining with CellROX Green Reagent (Life Technologies) and an Annexin V-Cy3 detection kit (PromoKine) were used to evaluate the generation of oxidative stress and apoptosis. One week after FG labeling, 2 μl of AAPH 30 mM was injected in the mice intravitreally. Twenty-two hours later, 1 μl of 100 μM CellROX and 25×10^{-3} μg of Annexin V-Cy3 were injected intravitreally under general anesthesia (performed with ketamine and xylazine).

The retinas were harvested 24 h after the injection of AAPH, fixed with 4% PFA for 2 h and flat-mounted. The fluorescence of the reagents was evaluated with a confocal laser microscope (LSM780, Carl Zeiss, Oberkochen, Germany).

2.5. Detection of AAPH-induced calpain activation in the RGCs

To investigate the localization of calpain activation, we stained the retinas with a fluorogenic substrate [15]. To identify the RGCs, retrograde labeling was performed as described above, with DiI (CellTracker CM-DiI, Life Technologies). One week after retrograde labeling, the left eye of each mouse received an intravitreal injection of 2 μl of 30 mM AAPH, under anesthesia. As a control, the contralateral eye was injected with 2 μl DPBS. Twenty-one hours later, both eyes received intravitreal injections of fluorogenic cell-permeable calpain substrate ((DABCYL)-TPLK~SPPPSPRE (EDANS)-RRRRRRR-NH₂ calpain substrate IV, Millipore). The retinas were harvested 24 h after AAPH injection, immediately fixed with 4% PFA for 2 h and flat mounted. The fluorescence of the fluorogenic substrate, representing the activation of calpain, was evaluated with an Axiovert 200 microscope (Carl Zeiss, Oberkochen, Germany).

2.6. Statistical analysis

Statistical analysis was performed using JMP pro 10.02 (SAS Institute Inc.) software for Windows. Continuous variables were expressed as mean values \pm standard deviation. The *t*-test was used to analyze differences between pairs of groups. Multiple comparisons were done using ANOVA with Dunnett's post hoc analysis. The level of significance was 0.05 in all statistical tests.

3. Results

3.1. The effect of AAPH treatment on RGC survival

To investigate the effect of AAPH-induced oxidative stress on RGC survival, we performed the intravitreal injection of AAPH (30 mM, 2 μ l) or DPBS (2 μ l) in the mice. Seven days after the administration of AAPH, we counted the number of FG-labeled RGCs and found that they had significantly decreased (control: 3806.7 ± 575.2 RGCs/mm², AAPH: 3156.1 ± 371.2 RGCs/mm², $P < 0.01$, $n = 8$, Fig. 1). This finding indicated that the administration of AAPH could induce significant RGC death.

3.2. Detecting oxidative stress, calpain activation and apoptosis in the RGCs after AAPH treatment

In the control group, CellROX and Annexin V signals in the retina were not co-localized. However, in the AAPH-treated group, CellROX and Annexin V signals were co-localized with the FG-labeled RGCs 24 h after AAPH injection (Fig. 2A). This result indicated that oxidative stress occurred in the RGCs after AAPH treatment. Next, in order to confirm the activation of calpain in the RGCs, we used a fluorogenic calpain substrate to visualize calpain activation (Fig. 2B). The expression of the fluorogenic calpain substrate was co-localized with the DiI signal. This result indicated that calpain activation occurred in the RGCs 24 h after the administration of AAPH. In the control eyes, by contrast, we did not observe calpain activation in the RGCs.

3.3. Blocking calpain activation prevents RGC death caused by oxidative stress

To investigate the relationship between calpain activation and AAPH treatment, we performed an immunoblot analysis. This analysis showed that the band of cleaved α -fodrin, a substrate of calpain, was significantly detectable 24 h after AAPH administration, but not after 3 or 6 h (Fig. 3A). The intensity of the band increased

significantly, by more than twofold. It is known that activated calpain can cleave α -fodrin to a size of 145 kDa. This result indicated that AAPH was able to induce RGC death through oxidative stress, and suggested that it could be related to calpain activation. We confirmed this result by treating the AAPH-injected eyes with SNJ-1945, a specific calpain inhibitor (Fig. 3B). SNJ-1945 prevented the cleavage of α -fodrin that occurred 24 h after AAPH injection (SNJ-1945 treatment: 0.6 ± 0.3 -fold change vs. no treatment, $P < 0.05$, $n = 4$).

These results showed that AAPH-induced oxidative stress in the RGCs caused calpain activation and subsequent RGC death. In order to obtain further confirmation of these results, we performed the intraperitoneal administration of SNJ-1945, and found that it significantly reduced RGC death in our animal model (AAPH: 3369.8 ± 216.0 RGCs/mm², AAPH+SNJ-1945: 3817.8 ± 469.6 RGCs/mm², $P < 0.05$, Fig. 4).

4. Discussion

In this study, we used the intravitreal administration of AAPH, a free radical generator, to establish an animal model of the oxidative stress that occurs in the RGCs in neurodegenerative diseases of the eye. We found that oxidative stress in this model was associated with calpain activation in the retina and RGC death after 7 days. Moreover, AAPH administration successfully induced oxidative stress, confirmed by the finding that CellROX and Annexin V-Cy3 signals were co-localized in FG-labeled RGCs. AAPH administration also led to the activation of calpain in the retina after 24 h, confirmed by an immunoblot analysis. Moreover, the intraperitoneal administration of SNJ-1945 had a neuroprotective effect *in vivo*, preventing the cleavage of α -fodrin and RGC death after AAPH administration. These results indicate that oxidative stress-induced RGC death is mediated in part through the calpain pathway.

Previously, AAPH has been used to induce oxidative stress in non-RGC retinal cells, such as the photoreceptors, *in vitro* [16,17]. Furthermore, it has been reported that oxidative stress can induce apoptosis of the RGCs *in vitro* [18,19]. Our previous work has also demonstrated the importance of oxidative stress, by showing that mice deficient in Nrf2, a key transcription factor regulating antioxidant genes, had significantly fewer surviving FG-labeled RGCs after NC than wild-type mice [6], and that CDDO-Im, an extremely potent Nrf2 activator, prevented NC-induced RGC death *in vivo* [20]. Therefore, we expected that oxidative stress induced by AAPH would cause equivalently significant damage to the RGCs *in vivo*. Our results confirmed these expectations, showing that AAPH administration reduced the number of RGCs by 17% after 7 days.

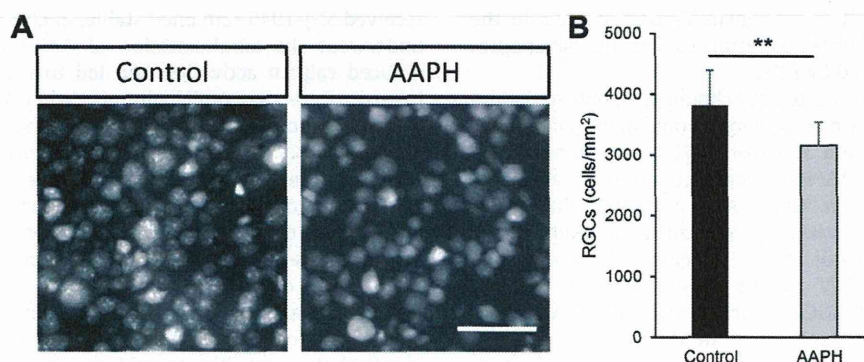


Fig. 1. Comparison of RGC density in the control and AAPH-treated groups. (A) Representative appearance of RGCs in flat-mounted retinas with quantitative data on RGC density 7 days after the intravitreal administration of AAPH. (B) Comparison of RGC density, determined by RGC counting, in the control and AAPH-treated groups. RGC density decreased significantly, by 17%, in the AAPH treatment group compared to the control group. RGC: retinal ganglion cell; scale bar: 50 μ m, error bar: standard deviation; *t*-test, ** $P < 0.01$.

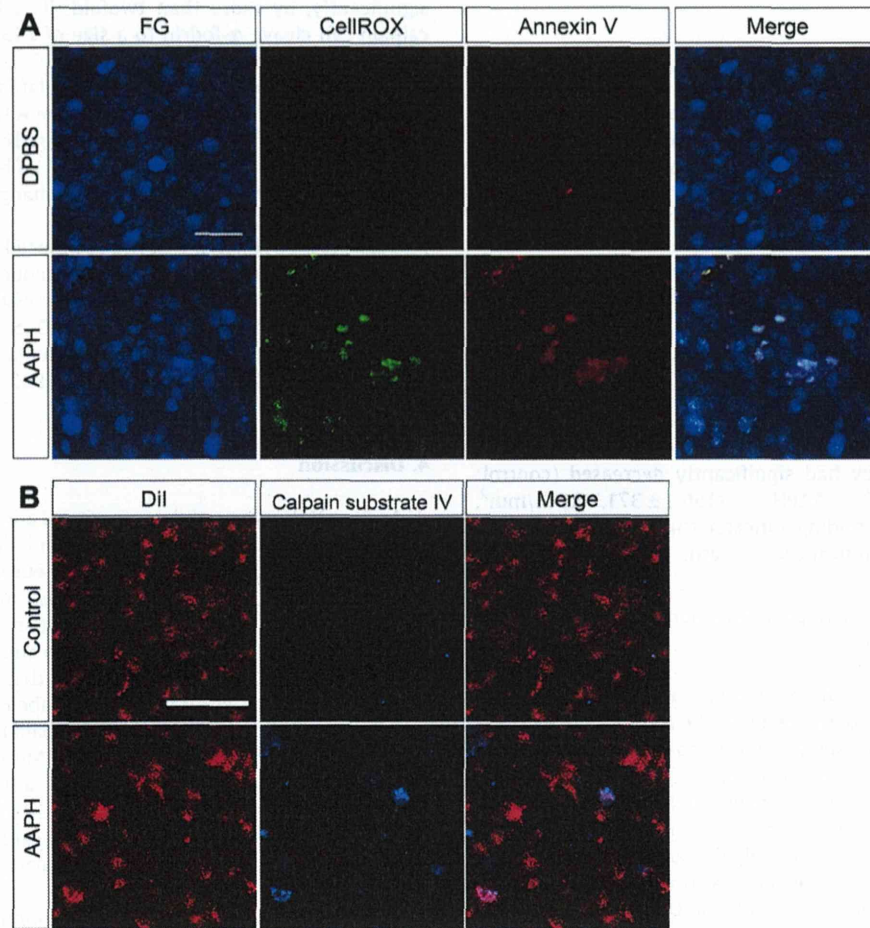


Fig. 2. Oxidative stress, calpain activation and apoptosis 24 h after AAPH administration. (A) Representative images of flat-mounted retinas showing CellROX and Annexin V signals, used to detect oxidative stress and apoptosis in the RGCs. CellROX and Annexin V signals were co-localized in the AAPH-treated retinas, while the DPBS-treated retinas showed no CellROX or Annexin V signals. (B) Representative appearance of Dil-labeled RGCs in flat-mounted retinas, with calpain substrate IV signals showing calpain activation. Twenty-four hours after AAPH administration, the control retinas showed no calpain substrate IV signals, while the AAPH-treated retinas showed co-localized calpain substrate IV signals and Dil-labeled RGCs. Scale bar: 50 μ m.

Previous studies have reported that mitochondrial-derived death signaling is a major pathway of axonal damage-induced RGC death [21,22]. Mitochondria play an important role in the regulation of cell viability [23]. Oxidative stress induces mitochondrial-derived reactive oxygen species (ROS) generation and disturbs the function of calcium buffering [24–26]. To explore the mechanism of RGC death in the current investigation, we therefore assessed CellROX and Annexin V-positive RGCs in the AAPH-treated retinas, and obtained results suggesting that apoptosis of the RGCs was induced by ROS.

ROS induce the processing of mitochondrial apoptosis-inducing factor (AIF) and increase sensitivity to mitochondrial calpain, resulting in AIF cleavage and apoptosis [27]. Using immunoblotting, we investigated the AAPH-induced activation of calpain by testing for cleaved α -fodrin. Our results indicated that AAPH treatment induced fragmentation of α -fodrin as a result of calpain activation in the overall retina. Moreover, the co-localization of calpain substrate IV signals, which represent calpain activation, and Dil-labeled RGCs confirmed that calpain was activated in the RGCs. This suggests that the calpain pathway may be activated by an increased inflow of Ca^{2+} through Ca^{2+} channels under pathological conditions such as oxidative stress. Moreover, previous studies have shown that oxidative stress increases intracellular free Ca^{2+} levels, and activates Ca^{2+} -depen-

dent enzymes [27–29]. These data suggest that oxidative stress and dysfunctional calcium buffering in the mitochondria may be major links with calpain activation in the retina, a finding that is consistent with our results.

Additionally, SNJ-1945 administration demonstrated a potent neuroprotective effect against AAPH-induced RGC death. Indeed, the number of RGCs after AAPH administration in the mice that received SNJ-1945 remained stable, in contrast with the mice that underwent the administration of AAPH and vehicle. SNJ-1945 reduced calpain activation and led to reduced cleaved α -fodrin intensity 24 h after AAPH administration. This result is consistent with past reports showing that oxidative stress caused calpain activation in RGCs that had been isolated *in vitro* [30] and that SNJ-1945 had a neuroprotective effect in the RGCs [7,31]. Here, using our *in vivo* model, we showed that the activation of calpain occurs downstream of oxidative stress, and that the inhibition of calpain activation was an effective way of preventing oxidative stress-induced RGC damage.

The animal model of oxidative stress described here may be appropriate for some purposes, such as investigating drug effects in cells that are sensitive to oxidative stress, but for other purposes, the intensity of AAPH-induced damage may be insufficient. Opportunities to refine this animal model therefore include the use of other ROS generators, such as rotenone [32] and paraquat, which

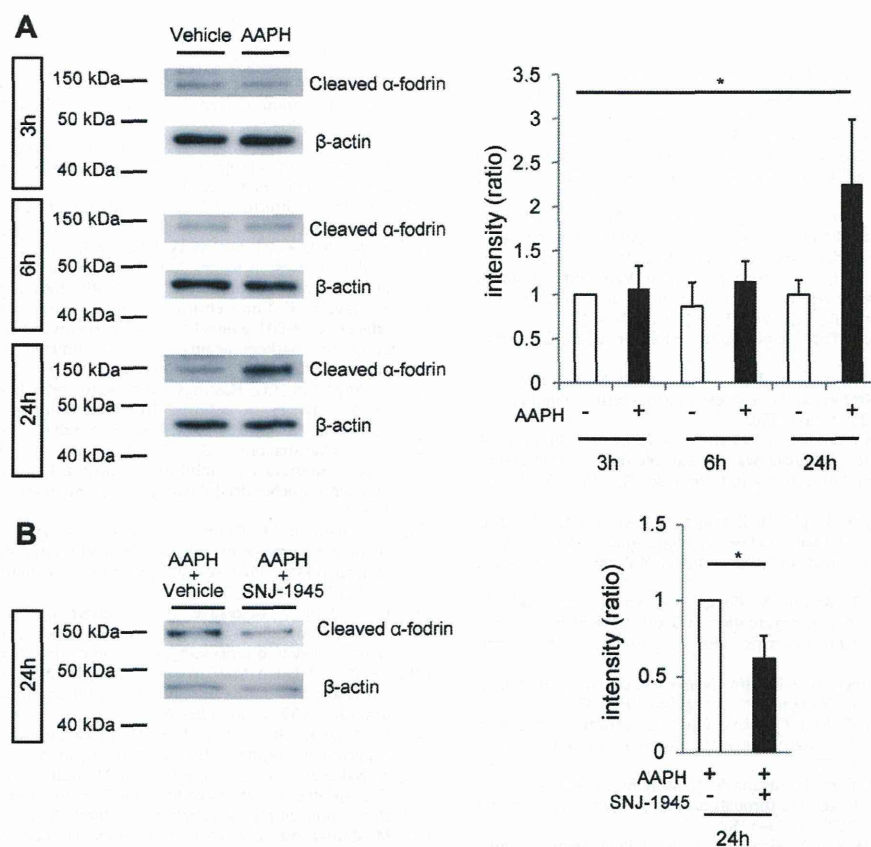


Fig. 3. Immunoblot analysis of calpain activation in mouse retinas after AAPH treatment. (A) Representative immunoblots and bar graphs showing the expression level of cleaved α -fodrin at each time point, compared with cleaved α -fodrin expression after 3 h in vehicle-treated retinas. β -Actin was used as an internal standard for the assessment of α -fodrin. The intensity of cleaved α -fodrin, i.e., of the 145-kDa fragments produced by activated calpain, was significantly higher 24 h after AAPH administration than after vehicle. Error bar: standard deviation ANOVA with Dunnett's post hoc analysis; $*P < 0.05$. (B) Representative immunoblots showing calpain activation 24 h after AAPH administration, with or without SNJ-1945. The bar graphs show the expression level of cleaved α -fodrin in the SNJ-1945-treated and -untreated retinas. These results show that SNJ-1945 attenuated the intensity of α -fodrin cleavage. Error bar: standard deviation; t -test, $*P < 0.05$.

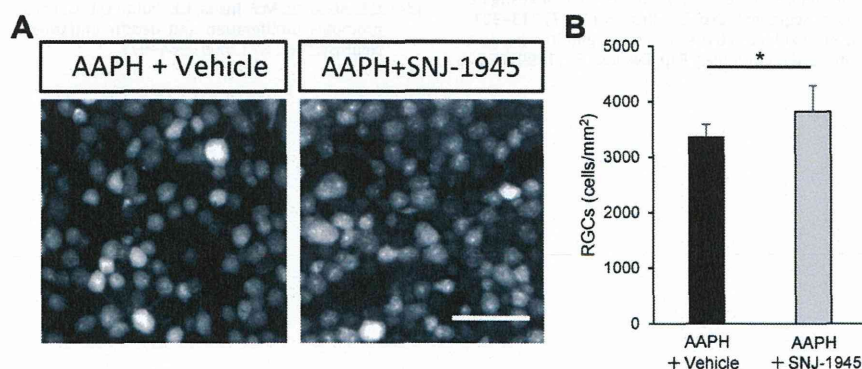


Fig. 4. Comparison of RGC density with and without SNJ-1945. (A) Representative appearance of RGCs in flat-mounted retinas 7 days after the intravitreal administration of AAPH. (B) Comparison of RGC density, determined by RGC counting, with and without SNJ-1945. RGC density was significantly higher with SNJ-1945, suggesting that SNJ-1945 protected the RGCs from AAPH-induced damage. Scale bar: 50 μ m. Error bar: standard deviation; t -test, $*P < 0.05$.

have a cytotoxic effect in retinal cells and dopaminergic cells [33,34].

In conclusion, we successfully established an *in vivo* model of oxidative stress in the RGCs with AAPH, and used this model to demonstrate that the calpain pathway is activated downstream of oxidative stress. Furthermore, suppressing calpain activation reduced RGC death in our model, suggesting that it may be a good candidate for neuroprotection therapy. Our findings may also be

useful in future investigations of oxidative stress-related ocular diseases, such as glaucoma and diabetic axonal atrophy.

Acknowledgments

We thank Ms. Kaori Hanekawa for technical assistance and Mr. Tim Hilts for editing this document. We also thank Senju Pharmaceutical Co., Ltd. for the generous gift of SNJ-1945.

References

- [1] J. Lee, M. Kannagi, R.J. Ferrante, N.W. Kowall, H. Ryu, Activation of Ets-2 by oxidative stress induces Bcl-xL expression and accounts for glial survival in amyotrophic lateral sclerosis, *FASEB J.* 23 (2009) 1739–1749.
- [2] M. Ramamoorthy, P. Sykora, M. Scheibye-Knudsen, C. Dunn, C. Kasmer, Y. Zhang, K.G. Becker, D.L. Croteau, V.A. Bohr, Sporadic Alzheimer disease fibroblasts display an oxidative stress phenotype, *Free Radic. Biol. Med.* 53 (2012) 1371–1380.
- [3] D.H. Choi, A.C. Cristovao, S. Guhathakurta, J. Lee, T.H. Joh, M.F. Beal, Y.S. Kim, NADPH oxidase 1-mediated oxidative stress leads to dopamine neuron death in Parkinson's disease, *Antioxid. Redox Signal.* 16 (2012) 1033–1045.
- [4] K.N. Engin, B. Yemisci, U. Yigit, A. Agachan, C. Coskun, Variability of serum oxidative stress biomarkers relative to biochemical data and clinical parameters of glaucoma patients, *Mol. Vis.* 16 (2010) 1260–1271.
- [5] A. Izzotti, A. Bagnis, S.C. Sacca, The role of oxidative stress in glaucoma, *Mutat. Res.* 612 (2006) 105–114.
- [6] N. Himori, K. Yamamoto, K. Maruyama, M. Ryu, K. Taguchi, M. Yamamoto, T. Nakazawa, Critical role of Nrf2 in oxidative stress-induced retinal ganglion cell death, *J. Neurochem.* 127 (2013) 669–680.
- [7] M. Ryu, M. Yasuda, D. Shi, A.Y. Shanab, R. Watanabe, N. Himori, K. Omodaka, Y. Yokoyama, J. Takano, T. Saido, T. Nakazawa, Critical role of calpain in axonal damage-induced retinal ganglion cell death, *J. Neurosci. Res.* 90 (2012) 802–815.
- [8] C.Y. Wang, J.W. Xie, T. Wang, Y. Xu, J.H. Cai, X. Wang, B.L. Zhao, L. An, Z.Y. Wang, Hypoxia-triggered m-calpain activation evokes endoplasmic reticulum stress and neuropathogenesis in a transgenic mouse model of Alzheimer's disease, *CNS Neurosci. Ther.* (2013).
- [9] T. Nakazawa, M. Shimura, R. Mourin, M. Kondo, S. Yokokura, T.C. Saido, K. Nishida, S. Endo, Calpain-mediated degradation of G-substrate plays a critical role in retinal excitotoxicity for amacrine cells, *J. Neurosci. Res.* 87 (2009) 1412–1423.
- [10] A. Camins, E. Verdaguer, J. Folch, M. Pallas, Involvement of calpain activation in neurodegenerative processes, *CNS Drug Rev.* 12 (2006) 135–148.
- [11] R. Piga, Y. Saito, Y. Yoshida, E. Niki, Cytotoxic effects of various stressors on PC12 cells: involvement of oxidative stress and effect of antioxidants, *Neurotoxicology* 28 (2007) 67–75.
- [12] T. Nakazawa, M. Shimura, S. Endo, H. Takahashi, N. Mori, M. Tamai, N-methyl-D-aspartic acid suppresses Akt activity through protein phosphatase in retinal ganglion cells, *Mol. Vis.* 11 (2005) 1173–1182.
- [13] T. Nakazawa, M. Shimura, M. Ryu, K. Nishida, G. Pages, J. Pouyssegur, S. Endo, ERK1 plays a critical protective role against N-methyl-D-aspartate-induced retinal injury, *J. Neurosci. Res.* 86 (2008) 136–144.
- [14] T. Nakazawa, M. Takeda, G.P. Lewis, K.S. Cho, J. Jiao, U. Wilhelmsson, S.K. Fisher, M. Pekny, D.F. Chen, J.W. Miller, Attenuated glial reactions and photoreceptor degeneration after retinal detachment in mice deficient in glial fibrillary acidic protein and vimentin, *Invest. Ophthalmol. Vis. Sci.* 48 (2007) 2760–2768.
- [15] Z. Banoczi, A. Alexa, A. Farkas, P. Friedrich, F. Hudecz, Novel cell-penetrating calpain substrate, *Bioconjug. Chem.* 19 (2008) 1375–1381.
- [16] S.A. Keys, E. Boley, W.F. Zimmerman, A model membrane system to investigate antioxidants in bovine rod outer segments, *Exp. Eye Res.* 64 (1997) 313–321.
- [17] S.A. Keys, W.F. Zimmerman, Antioxidant activity of retinol, glutathione, and taurine in bovine photoreceptor cell membranes, *Exp. Eye Res.* 68 (1999) 693–702.
- [18] Z.K. Yu, Y.N. Chen, M. Aihara, W. Mao, S. Uchida, M. Araie, Effects of beta-adrenergic receptor antagonists on oxidative stress in purified rat retinal ganglion cells, *Mol. Vis.* 13 (2007) 833–839.
- [19] P. Maher, A. Hanneken, The molecular basis of oxidative stress-induced cell death in an immortalized retinal ganglion cell line, *Invest. Ophthalmol. Vis. Sci.* 46 (2005) 749–757.
- [20] N. Himori, K. Yamamoto, K. Maruyama, M. Ryu, K. Taguchi, M. Yamamoto, T. Nakazawa, Critical role of Nrf2 in oxidative stress-induced retinal ganglion cell death, *J. Neurochem.* (2013).
- [21] S. Chierzi, E. Strettoi, M.C. Cenni, L. Maffei, Optic nerve crush: axonal responses in wild-type and bcl-2 transgenic mice, *J. Neurosci.* 19 (1999) 8367–8376.
- [22] X. Qi, A.S. Lewin, L. Sun, W.W. Hauswirth, J. Guy, Suppression of mitochondrial oxidative stress provides long-term neuroprotection in experimental optic neuritis, *Invest. Ophthalmol. Vis. Sci.* 48 (2007) 681–691.
- [23] R.L. Jayaraj, K. Tamilselvan, T. Manivasagam, N. Elangovan, Neuroprotective effect of CNB-001, a novel pyrazole derivative of curcumin on biochemical and apoptotic markers against rotenone-induced SK-N-SH cellular model of Parkinson's disease, *J. Mol. Neurosci.* (2013).
- [24] I.J. Reynolds, T.G. Hastings, Glutamate induces the production of reactive oxygen species in cultured forebrain neurons following NMDA receptor activation, *J. Neurosci.* 15 (1995) 3318–3327.
- [25] S.C. Chattipakorn, S. Thummasorn, J. Sanit, N. Chattipakorn, Phosphodiesterase-3 inhibitor (cilostazol) attenuates oxidative stress-induced mitochondrial dysfunction in the heart, *J. Geriatr. Cardiol.* 11 (2014) 151–157.
- [26] I.B. Zavodnik, I.K. Dremza, V.T. Cheshchevik, E.A. Lapshina, M. Zamarawa, Oxidative damage of rat liver mitochondria during exposure to t-butyl hydroperoxide. Role of Ca(2+) ions in oxidative processes, *Life Sci.* 92 (2013) 1110–1117.
- [27] E. Norberg, V. Gogvadze, H. Vakifahmetoglu, S. Orrenius, B. Zhivotovskiy, Oxidative modification sensitizes mitochondrial apoptosis-inducing factor to calpain-mediated processing, *Free Radic. Biol. Med.* 48 (2010) 791–797.
- [28] S.K. Ray, M. Fidan, M.W. Nowak, G.G. Wilford, E.L. Hogan, N.L. Banik, Oxidative stress and Ca²⁺ influx upregulate calpain and induce apoptosis in PC12 cells, *Brain Res.* 852 (2000) 326–334.
- [29] M. Azuma, T.R. Shearer, The role of calcium-activated protease calpain in experimental retinal pathology, *Surv. Ophthalmol.* 53 (2008) 150–163.
- [30] M. Nakayama, M. Aihara, Y.N. Chen, M. Araie, K. Tomita-Yokotani, T. Iwashina, Neuroprotective effects of flavonoids on hypoxia-, glutamate-, and oxidative stress-induced retinal ganglion cell death, *Mol. Vis.* 17 (2011) 1784–1793.
- [31] M. Shimazawa, S. Suemori, Y. Inokuchi, N. Matsunaga, Y. Nakajima, T. Oka, T. Yamamoto, H. Hara, A novel calpain inhibitor, ((1S)-1-(((1S)-1-Benzyl-3-cyclopropylamino-2,3-di-oxopropyl)amino)carbonyl)-3-methylbutyl)carbamic acid 5-methoxy-3-oxapentyl ester (SNJ-1945), reduces murine retinal cell death in vitro and in vivo, *J. Pharmacol. Exp. Ther.* 332 (2010) 380–387.
- [32] X. Zhang, D. Jones, F. Gonzalez-Lima, Mouse model of optic neuropathy caused by mitochondrial complex I dysfunction, *Neurosci. Lett.* 326 (2002) 97–100.
- [33] H. Li, S. Wu, Z. Wang, W. Lin, C. Zhang, B. Huang, Neuroprotective effects of tert-butylhydroquinone on paraquat-induced dopaminergic cell degeneration in C57BL/6 mice and in PC12 cells, *Arch. Toxicol.* 86 (2012) 1729–1740.
- [34] C.E. Abraham, M.F. Insua, L.E. Politi, O.L. German, N.P. Rotstein, Oxidative stress promotes proliferation and dedifferentiation of retina glial cells in vitro, *J. Neurosci. Res.* 87 (2009) 964–977.

RNA Sequence Reveals Mouse Retinal Transcriptome Changes Early after Axonal Injury

Masayuki Yasuda, Yuji Tanaka, Morin Ryu, Satoru Tsuda, Toru Nakazawa*

Department of Ophthalmology, Tohoku University Graduate School of Medicine, Sendai, Japan

Abstract

Glaucoma is an ocular disease characterized by progressive retinal ganglion cell (RGC) death caused by axonal injury. However, the underlying mechanisms involved in RGC death remain unclear. In this study, we investigated changes in the transcriptome profile following axonal injury in mice (C57BL/6) with RNA sequencing (RNA-seq) technology. The experiment group underwent an optic nerve crush (ONC) procedure to induce axonal injury in the right eye, and the control group underwent a sham procedure. Two days later, we extracted the retinas and performed RNA-seq and a pathway analysis. We identified 177 differentially expressed genes with RNA-seq, notably the endoplasmic reticulum (ER) stress-related genes *Atf3*, *Atf4*, *Atf5*, *Chac1*, *Chop*, *Egr1* and *Trb3*, which were significantly upregulated. The pathway analysis revealed that ATF4 was the most significant upstream regulator. The antioxidative response-related genes *Hmox1* and *Srxn1*, as well as the immune response-related genes *C1qa*, *C1qb* and *C1qc*, were also significantly upregulated. To our knowledge, this is the first reported RNA-seq investigation of the retinal transcriptome and molecular pathways in the early stages after axonal injury. Our results indicated that ER stress plays a key role under these conditions. Furthermore, the antioxidative defense and immune responses occurred concurrently in the early stages after axonal injury. We believe that our study will lead to a better understanding of and insight into the molecular mechanisms underlying RGC death after axonal injury.

Citation: Yasuda M, Tanaka Y, Ryu M, Tsuda S, Nakazawa T (2014) RNA Sequence Reveals Mouse Retinal Transcriptome Changes Early after Axonal Injury. PLOS ONE 9(3): e93258. doi:10.1371/journal.pone.0093258

Editor: Richard Libby, University of Rochester, United States of America

Received: November 16, 2013; **Accepted:** March 4, 2014; **Published:** March 27, 2014

Copyright: © 2014 Yasuda et al. This is an open-access article distributed under the terms of the Creative Commons Attribution License, which permits unrestricted use, distribution, and reproduction in any medium, provided the original author and source are credited.

Funding: This study was supported in part by Grants-in-Aid from the Ministry of Education, Science and Technology of Japan (24659756 for T.N. and 40625513 for Y.T.) (<http://www.mext.go.jp/english/>). This study was also supported by JST Center for Revitalization Promotion (<http://www.jst.go.jp/fukkou/>), All Japan Coffee Association (<http://coffee.ajca.or.jp/news/othernews/h26josei>), Senju Pharmaceutical Co., Ltd. (<http://www.senju.co.jp/>) and NIDEK Co., Ltd. (<http://www.nidek.co.jp/index-j.html>). This study was also supported by the Great East Japan Earthquake Reconstruction Support project of the RIKEN Omics Science Center, the RIKEN Genome Analysis Service (GeNAS), Illumina Co. and CLC Bio Co. The funders had no role in study design, data collection and analysis, decision to publish, or preparation of the manuscript.

Competing Interests: This study was supported by donated funds from Senju Pharmaceutical Co., Ltd. and NIDEK Co., Ltd. This study was also supported by Illumina Co. and CLC Bio Co. as part of a Great East Japan Earthquake Reconstruction Support grant. This does not alter the authors' adherence to all the PLOS ONE policies on sharing data and materials.

* E-mail: ntoru@oph.med.tohoku.ac.jp

Introduction

Glaucoma is a leading cause of blindness worldwide [1]. It is characterized by glaucomatous optic neuropathy (GON), and is associated with optic nerve degeneration that results in progressive visual dysfunction [2]. In glaucoma patients, the number of retinal ganglion cells (RGCs) decreases due to axonal degeneration, resulting in visual dysfunction. Despite the attempts of many clinicians and scientists to identify the molecular mechanisms of pathogenesis in glaucoma, they are not yet well understood, possibly because of the multifactorial nature of glaucoma [3].

High intraocular pressure (IOP) is widely recognized as a major risk factor for glaucoma, and treatment to lower IOP is currently the only method that evidence has shown to prevent the progression of the disease [4]. Recently, many varieties of IOP-lowering eye drops have become clinically available to treat glaucoma. However, substantial reductions in IOP, up to 30%, fail to halt the progress of visual dysfunction in some patients, particularly those with normal tension glaucoma (NTG) [5]. In addition to IOP, risk factors for NTG include age, myopia [6], parapapillary atrophy (PPA) [7] and reduced ocular blood flow [8]. There is thus a necessity for further investigation of these IOP-

independent mechanisms, and the development of new neuroprotective drug targets for glaucoma.

Many recent investigations have led to a growing understanding of the underlying mechanism of RGC death in glaucoma, which previous studies had found to be induced by axonal injury to the lamina cribrosa [3]. However, those studies were mainly designed around approaches that focused on only a few pathways [9,10]. In order to overcome the heterogeneous and multifactorial nature of glaucoma and find novel critical molecular targets for treatment, it is necessary to use a global approach (i.e., one including the transcriptome and proteome).

A simple animal model mimicking the pathogenesis of glaucoma is a useful tool in investigations of the mechanism of RGC death, because standard excisional biopsy is impossible in the case of the human retina [11]. In one of the most widely used models, optic nerve crush (ONC) is performed in mice to induce axonal injury, which is a contributor to the progression of RGC death in glaucoma [10,12–14]. Interestingly, in this model the number of RGCs is maintained for a short duration after ONC, and significant RGC loss is not observed until day 3 [10]. Significant axonal damage is known to occur in the retina before visual field defects become detectable [15]. It would therefore be very useful to develop diagnostic methods and drug targets that functioned in

these early stages of glaucoma. Analysis of post-ONC mouse retinas in the early stages of axonal injury, before RGC loss (i.e., on day 2), may give us valuable insights to help achieve this goal.

Microarray analysis is a common way to evaluate the expression level of large numbers of genes simultaneously. It has also been used to evaluate changes after axonal injury both in the retina in general and in isolated RGCs [16]. However, microarrays are only capable of measuring known transcripts, and do not allow the investigation of total genetic changes. By contrast, RNA sequencing (RNA-seq) is able to assess complete genes and splice variants, with a high degree of reproducibility that matches that of microarrays [17]. RNA-seq technology thus has the potential to give us very useful, detailed information on the mechanisms of disease, as well as unknown pathways and networks of disease, that may lead to the discovery of new treatment strategies.

The purpose of this study was thus to use RNA-seq to investigate the molecular mechanisms of damage in the early stages of the response to axonal injury, before the onset of RGC death. We believe that our study may open new avenues of investigation into treatment strategies for axonal damage associated with ocular diseases, especially glaucoma.

Results

RNA-seq analysis and global gene expression profiles in axonal injury

In order to investigate the transcriptome profile at an early stage after axonal injury, but before significant RGC loss [10], we performed an RNA-seq analysis of mouse retinas harvested 2 days after ONC or sham operations. In order to obtain triplicate results, three samples were obtained from each group, each sample being a combination of material from six unique retinas. Each of these samples was sequenced on one lane of the Illumina HiSeq2000 platform (Illumina, San Diego, CA). All sequence reads were mapped to the reference genome (NCBI37/mm9) with CLC Genomics Workbench (version 6.0.1) (CLC Bio, Aarhus, Denmark) [18,19]. The total number of reads per lane was approximately 400 million, and the total number of reads per sample ranged from 62.9 to 70.3 million. An average 73.8% of total reads were mapped in pairs to the reference genome (Table S1). Detailed mapping statistics are listed on Table S2. To determine the expression level of various genes and compare them between samples, we used variable RPKM (reads per kilobase of exon per million mapped reads) [20]. To examine the overall distribution of gene expression values, we created box plots of RPKM expression values with CLC Genomics Workbench (Figure 1A). Overall RPKM expression values were similar in each sample. We excluded genes that did not have a mean RPKM > 0.3 in at least one group, in order to remove background noise [21]. The number of genes with a mean RPKM > 0.3 in at least one group was 13160. These were used for the differential gene expression analysis [19]. Fold change (FC) differences between the mice that underwent ONC and those that underwent a sham operation were calculated. The Student's t-test was performed to compare the groups with R software (version 3.0.1) [22]. *P*-values were adjusted for multiplicity with the Bioconductor package *qvalue* to control the false discovery rate (FDR) [23]. Differentially expressed genes (DEGs) were defined as those with $|FC| > 1.5$ and $FDR < 0.1$ [24]. It is known that the cells affected by ONC are mainly RGCs. The abundance ratio of RGCs in retinal tissue has been reported to very low (less than 0.5%) [25]. Furthermore, an approximately 1.5 to 2-fold increase in gene expression (e.g., in *Jun*, *Jund* and *Gadd45a*) has been reported to be a significant change in a previous analysis of changes in the entire retina after optic

nerve crush [26]. We therefore applied this relatively lower cutoff ($|FC| > 1.5$ and $FDR < 0.1$) in the current study. We created a volcano plot showing DEGs as red dots with the *ggplot2* package in R software [27] (Figure 1B). We also conducted a hierarchical clustering analysis of DEGs from all samples with Ward's method of Euclidean distances [28], and created a heatmap with the *heatmap.2* function of the *gplots* package of R software [29]. The results indicated that gene expression was similar in each group (Figure 1C).

Differentially expressed genes after ONC

The triplicate samples from the ONC and sham groups were assayed for DEGs, and 177 DEGs (132 up- and 45 downregulated genes) were identified (Table S3). The 10 most up- and downregulated genes are listed in Table 1. The expression changes of known RGC markers and axon regeneration markers [16,30,31] are summarized in Table 2. We found that the following RGC markers were significantly downregulated 2 days after ONC: *Nefh* (−2.24-fold), *Pou4f1* (−1.54-fold), *Pou4f2* (−2.40-fold), *Rbpms* (−1.62-fold) and *Sncg* (−1.77-fold). Interestingly, the expression of *Thy1* and *Pou4f3* did not change significantly at this time point (day 2). Generally, the expression of *Thy1* begins to decrease 3 days after axotomy in rats [32]. The following axon regeneration markers were significantly upregulated after ONC: *Gap43* (1.53-fold) and *Sprr1a* (23.81-fold).

A review of the published literature revealed that the following sets of endoplasmic reticulum (ER) stress-related genes have been shown to be significantly upregulated 2 days after ONC: *Atf3*, *Atf4*, *Atf5*, *Chac1*, *Ddit3*, *Egr1*, *Trib3* [33–35] (Table 2).

Significant networks and biological functions after ONC revealed by pathway analysis

To investigate the pathways involved in axonal injury, the DEG dataset was uploaded to Ingenuity Pathway Analysis (IPA, Ingenuity Systems, Redwood City, CA) and mapped to the Ingenuity Pathways Knowledge Base (IPKB) [36]. The 2 most significant networks are shown in Figure 2. Network 1 (Figure 2A) was associated with the “Cell Death and Survival”, “Cancer” and “Cell Morphology” pathways. Network 2 (Figure 2B) was associated with the “Neurological Disease”, “Nervous System Development and Function” and “Tissue Morphology” pathways. Table 3 lists the 5 most significant molecular and cellular functions. The most significant biofunction response, according to IPA, was for the “Cell Death and Survival” pathway, which involved 45 genes (Table S4).

RT-PCR validation of RNA-seq data

To validate the RNA-seq findings, we prepared new mouse retinas in each group, and performed RT-PCR on these new groups of retinas. We selected 14 genes (*Sprr1a*, *Mmp12*, *Sox11*, *Atf3*, *Tnfrsf12a*, *Hmox1*, *Plat*, *Egr1*, *Atf5*, *Ddit3*, *Jun*, *Pou4f2*, *Nefh* and *Pou4f1*) involved in the “Cell Death and Survival” pathway, and examined changes in their expression with RT-PCR (Table 4). We found that results obtained with RT-PCR were similar to those obtained with RNA-seq.

Upstream analysis and global network interactions after axonal injury

In order to investigate molecular network interactions, IPA performed an upstream regulator analysis. Table 5 shows the transcription factors that IPA predicted to be upstream regulators. The most significant was ATF4, but TP53, nuclear factor (erythroid-derived 2)-like 2 (NFE2L2) and DNA-damage inducible